A piezoelectric shear stress sensor

Taeyang Kim[a], Aditya Saini[a], Jinwook Kim[a], Ashok Gopalarathnam[a], Yong Zhu[a],
Frank L. Palmieri[b], Christopher J. Wohl[b], and Xiaoning Jiang*[a]
[a]Dept. of Mechanical and Aerospace Engr., North Carolina State Univ., 911 Oval Drive, Raleigh, NC, USA 27695
[b]NASA Langley Research Center, 8 Lindbergh Way, Hampton, VA, USA 23681

ABSTRACT

In this paper, a piezoelectric sensor with a floating element was developed for shear stress measurement. The piezoelectric sensor was designed to detect the pure shear stress suppressing effects of normal stress generated from the vortex lift-up by applying opposite poling vectors to the piezoelectric elements. The sensor was first calibrated in the lab by applying shear forces and it showed high sensitivity to shear stress (=91.3 ± 2.1 pC/Pa) due to the high piezoelectric coefficients of PMN-33%PT (d_{31}=–1330 pC/N). The sensor also showed almost no sensitivity to normal stress (less than 1.2 pC/Pa) because of the electromechanical symmetry of the device. The usable frequency range of the sensor is 0-800 Hz.

Keywords: Piezoelectric sensor, shear stress, floating element, electromechanical symmetry

1. INTRODUCTION

The accurate measurement of the wall shear stress induced by the flow over a solid surface is useful for understanding the critical vehicle characteristics, such as lift, drag, and propulsion efficiency. Therefore, the ability to obtain quantitative, time-resolved shear stress measurements may elucidate complex physics and ultimately help engineers improve the performance of aerospace and naval vehicles.

Various measurement techniques have been used to determine the shear stress at the wall surface. For example, devices such as the Preston tube or the Stanton tube and the hot film anemometers allow the estimation of aerodynamic shear stresses with indirect techniques, through the measurement of a pressure gradient or a heat transfer, respectively[1,2]. However, they strongly depend on empirical laws, with no guarantee of their accuracy in flow circumstances.

Considering the limitations of the indirect methods, which strongly depend on empirical laws with no guarantee of their accuracy in the considered flow[3], direct methods present the more accurate and sound approach to measuring the shear stress in complex and poorly-understood flows[4] because the sensing element responds directly to shear forces with direct measurements. An example of a direct measurement method is the floating element sensor, which is based on measuring the displacement of a floating element that is flush with the flow. Capacitive[5,6] and piezoresistive[7,8] techniques as well as surface acoustic wave (SAW) devices[9,10] have been developed and used to measure the displacement of a floating element. However, the shear stress sensors fabricated through micro-machining have not yet received sufficient validation in a turbulent flow environment, so further advancement is still needed to obtain reliable, high resolution shear stress measurements that are applicable to a wide range of flows.

In this work, the floating element sensor, the direct technique, was developed for shear stress measurement with small size (10×10×20 mm^3), low cost and ease of fabrication. PMN-33%PT crystal was adopted in the sensor for its high piezoelectric coefficient (d_{31}=–1330 pC/N)[11,12]. The proposed sensor was specially designed not only to prevent the potential errors caused by the misalignments of the floating element with respect to the test plate, but also not to be affected by normal stresses generated from the vortex lift up through the electromechanical symmetry of the sensing structure. Thus, we hypothesize that our piezoelectric floating element sensor is able to measure the pure shear stress at the actual flow circumstance.

*xjiang5@ncsu.edu; phone 1 919-515-5240; fax 1 919-515-7968; http://www.mae.ncsu.edu/jiang/

2. SENSOR DESIGN AND FABRICATION

2.1 Design

In this work, the floating element sensing and direct piezoelectric effect were used as sensing mechanisms[13]. As illustrated in Fig. 1, the floating element slips according to the magnitude of the shear force. The slip of floating element induces the deflection (δ) of the bimorph piezoelectric structures in which piezoelectric bimorph bending consequently leads to the generation of electrical charge through the lateral piezoelectric effect quantified by the coefficient, d_{31}, of the piezoelectric plates. The use of two parallel bimorphs allows the sliding element to move parallel to the fixed one, preventing any rotation of the sensing armature that could perturb the flow. A shear stress is converted into a double-flexion deformation of the bimorphs. The tension and compression stresses are then distributed in a piezoelectric bimorph. Considering the double-flexion strain induced by the clamping, an alternative poling of each plate is necessary to prevent the electrical charge output from cancelling out, so each piezoelectric plate is divided into two parts in which the poling vectors P_1 and P_2 are opposite.

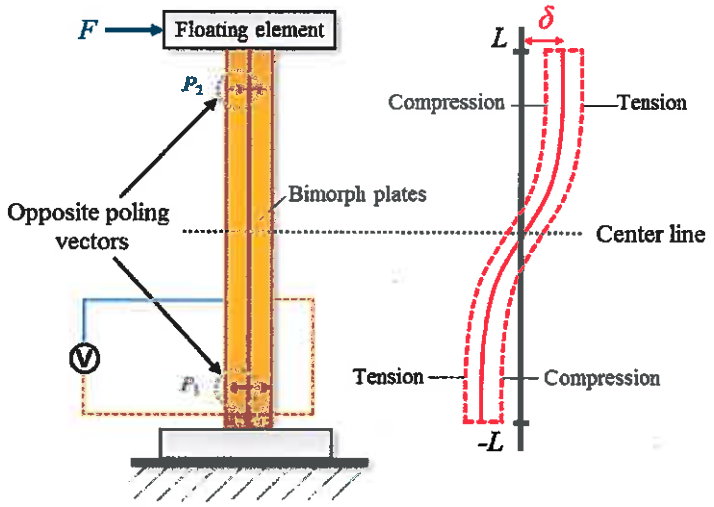

Figure 1. Configuration of deflection of bimorph structure

The measured slip of floating element and charge output can be used to calculate the calibrated shear stress by using the governing equation of direct piezoelectric effect[14,15], which can be derived on the basis of the thermodynamic analysis. In general, the constituent equations of the piezoelectric effect given in tensor form are expressed as,

$$S_{ij} = s^E_{ijkl} T_{kl} + d_{ijm} E_m \tag{1}$$

$$D_n = d_{nkl} T_{kl} + \epsilon^T_{nm} E_m \tag{2}$$

where S_{ij} is the strain, s^E_{ijkl} is the compliance at constant electric field, T_{kl} is the stress, d_{ijm} is the piezoelectric constant, E_m is the electric field, D_n is the dielectric displacement, ϵ^T_{nm} is the permittivity at constant stress.
In a series mode bimorph subjected to an external force (=F), the stress in the longitudinal direction (T_1) can be derived from a moment (=M) which is caused by an externally applied force,

$$M = F(L - x) \tag{3}$$

$$T_1 = \frac{3Mz}{2wh^3} = \frac{3F(L-x)z}{2wh^3} \tag{4}$$

where L, w and h are the length, width and height of the individual piezo-element, respectively. x and z are the distance from the fixed end and neutral axis of bimorph structure, respectively. Combining Eq. (4) with the piezoelectric effect induced stress, the total stress in each element becomes

$$T_1^U = \frac{d_{31}E_3}{s_{11}^E}\left(1 - \frac{3z^U}{2h}\right) - \frac{3F(L-x)z^U}{2wh^3}, \qquad 0 < z^U < h \tag{5}$$

$$T_1^L = \frac{d_{31}E_3}{s_{11}^E}\left(\frac{1}{2} - \frac{3z^L}{2h}\right) - \frac{3F(L-x)(z^L-h)}{2wh^3}, \qquad 0 < z^L < h \tag{6}$$

where the superscript U and L denote the upper and lower element of the bimorph. By applying Eqs. (5) and (6) into the energy density equation as the thermodynamic terms, the total energy (=U) in the beam is calculated as

$$U = U^U + U^L = \frac{F^2L^3s_{11}^E}{4wh^3} - \frac{3d_{31}VFL^2}{8h^2} + \frac{LwV^2}{4h}\left(\epsilon_{33}^T - \frac{d_{31}^2}{4s_{11}^E}\right) \tag{7}$$

It is known that the canonical conjugate of the force (=∂U/ ∂F) and the voltage (=∂U/ ∂V) are equal to the deflection at the tip (=δ) and the electric charge (=Q), so we can derive the constituent equations for the piezoelectric bimorph under an applied force as follows

$$\frac{\partial U}{\partial F} = \frac{s_{11}^E L^3 F}{2wh^3} - \frac{3d_{31}L^2V}{8h^2} \tag{8}$$

$$\frac{\partial U}{\partial V} = -\frac{3d_{31}L^2F}{8h^2} - \frac{LwV}{2h}\left(\epsilon_{33}^T - \frac{d_{31}^2}{4s_{11}^E}\right) \tag{9}$$

At last, considering the fixed-guided boundary condition, we can restate Eqs. (8) and (9) into matrix form

$$\begin{bmatrix} 2\delta \\ Q \end{bmatrix} = \begin{bmatrix} \frac{s_{11}^E L^3}{wh^3} & -\frac{3d_{31}L^2}{4h^2} \\ -\frac{3d_{31}L^2}{4h^2} & \frac{Lw}{h}\left(\epsilon_{33}^T - \frac{d_{31}^2}{4s_{11}^E}\right) \end{bmatrix} \begin{bmatrix} F \\ V \end{bmatrix} \tag{10}$$

Based on Eq. (10), the calculated shear stress sensitivity can be expressed as

$$S_{cal} = \frac{Q}{P}(V=0) = -\frac{3d_{31}L^2}{4h^2} \cdot A_{FE} \tag{11}$$

where A_{FE} is the surface area of floating element. So the sensitivity of bimorph piezoelectric sensor is proportional to the square of bimorph plate length and the surface area of floating element and inversely proportional to the square of the height of plate.

2.2 Fabrication

The floating element sensor was fabricated with a size of 10 × 10 × 20 mm^3. The fabrication process started from a shaping of PMN-33%PT plate with the dimension of 20 × 20 × 0.5 mm^3. After top and bottom surfaces of the PMN-33%PT plate were deposited with 200 nm-thick-Au-electrode by using e-beam evaporation, the plate was diced (16 × 2.5 mm^2) by using a mechanical dicing saw (Disco, DA320, Santa Clara, CA). Electrode gaps (= 1 mm) in the middle of plates were formed to apply opposite poling vectors in the plate (Fig. 2(a)). The poling condition of each plate was checked by an impedance-phase analyzer (Agilent 4294A, Agilent Technologies Inc., Santa Clara, CA). In Fig. 2(b), the number in a legend indicates

each side of four plates, i.e. 2 sides × 4 plates. All the impedance spectra showed an identical shape and the resonance frequency of ~4.5 MHz, which indicates that the opposite poling vectors in each plate were successfully applied. The poled PMN-PT plates were bonded as the series mode bimorphs using an epoxy resin (Epotek 301), since the series mode structure ensures the higher sensitivity of the sensors and the easier fabrication in comparison with the parallel mode connection[14]. As the last step, electrode gaps were connected using silver epoxy to draw all the electrical charge output together from the both sides of plates (Fig. 2(a)), then bimorph plates were clamped with the floating elements.

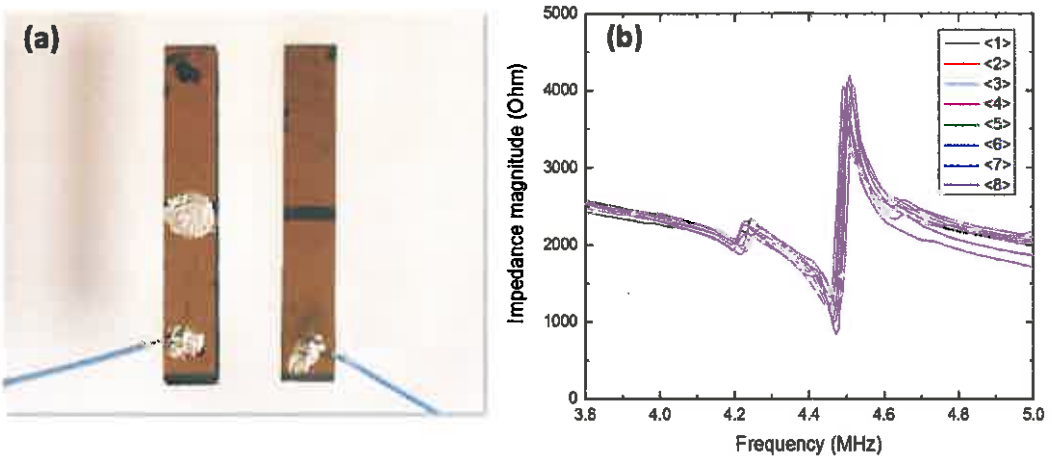

Figure 2. (a) Picture of bimorph plates with electrode gaps, (b) impedance spectra of both sides of the 4 plates

The sensor is consist of the floating element (top), the clamped element (bottom), two bimorph plates of PMN-33%PT crystal (Fig. 3). For the future wind tunnel test, several design considerations were applied to prevent the potential errors arise from the misalignments of the floating element with respect to the test plate. For example, gap size between the floating element and housing was precisely controlled (200 μm). According to Allen *et al.*, a sensor with a small gap size is much more prone to the misalignment error so the optimum ratio of gap (G) to length of floating element was determined to be 0.02.; and the lip size of the floating element was intentionally minimized (= 1 mm) based on the total height of the floating element (= 3 mm) to reduce the area on which the pressure had to act in the case of misalignment.[16–19]

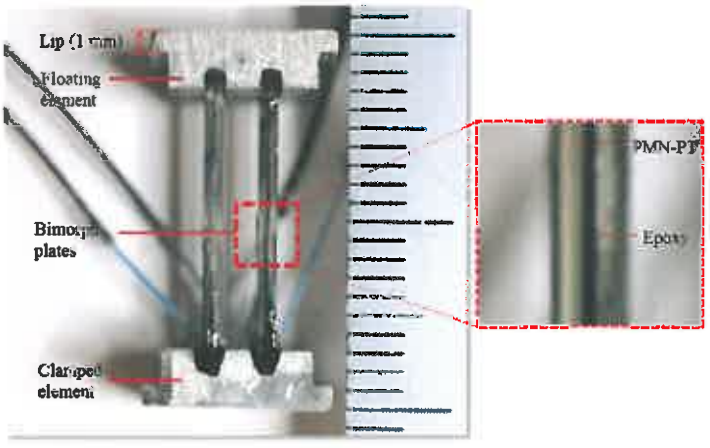

Figure 3. Configuration of PE sensor with bimorph structures

3. EXPERIMENTAL SETUP

For the characterization of the fabricated sensor, the clamped element of the sensor was fixed with a bench vise on a floating optical table (Newport, ATS, Irvine, CA) to eliminate the vibrational noise. Previously calibrated piezoelectric actuator (sensitivity of 5 μm/V) was used to apply dynamic forces to the prototype sensor. The actuator was excited by a function generator (Tektronix, Cary, NC) and a power amplifier (ValueTronics, Elgin, IL) applied vibration to sensor by contacting the probe at the floating element. The laser vibrometer (Polytec, Mooresville, NC) detected the amount of displacement of the floating element and the oscilloscope (Agilent Technologies, Santa Clara, CA) visualized the profile of displacement at the same time. Charge output generated from the deflection of bimorph plate were measured by a lock-in amplifier (Stanford Research Systems, Sunnyvale, CA) to filter out the noise signal. In this test, reference frequency was 1 Hz and excitation force was controlled by increasing voltage amplitude from the function generator in the range of 0.1 V to 1.0 V with 0.1 V sub-step. The dynamic calibration for the shear stress and normal stress were conducted by positioning the contact probe of actuator at the side (Fig.4 (a)) and on the top (Fig.4 (b)) of the floating element, respectively.

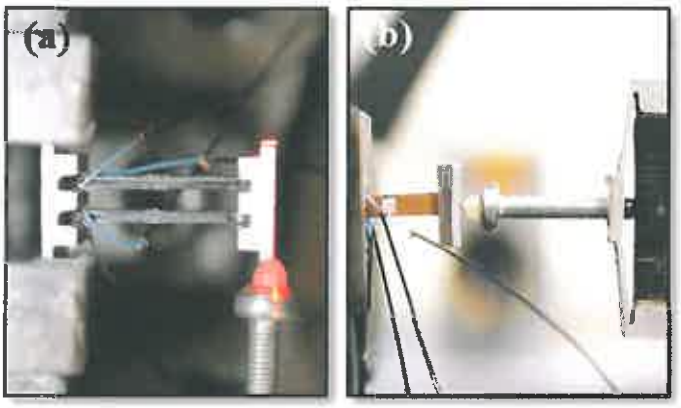

Figure 4. Calibration setup for (a) shear (b) normal stress

4. RESULTS AND DISCUSSION

The exciting shear force (F) from the actuator was converted into the applied shear stress (τ_w) by dividing it with a top area (A) of the floating element ($\tau_w = F/A$). As the shear stress increases, electrical charge output generated by the deflection of bimorph plates also increases and shows almost linear relationship with respect to the shear stresses (Fig. 5(a)). Based on the linear fitting equation, the resolution of the sensor can reach up to 0.5 Pa. Simulation results for verifying the shear stress distribution on the airfoil were conducted by using CFD XFOIL which is an airfoil design/analysis code (Fig. 5(b)). It shows that ranges of shear stress on the airfoil (range of 0.1-0.3 m from the leading edge) are 1.5-4.0 Pa in the velocity variation of 9.7 – 48.5 m/s, which indicates that proposed PE sensor is able to detect shear stress signal properly considering its resolution.

As for the calculated and measured sensor sensitivity toward the shear and normal stress, experimental shear stress sensitivity (=91.3 ± 2.1 pC/Pa) shows 10-12 % lower than the calculated value, which may be caused by inaccurate piezoelectric constants used in the calculation or the capacitance reduction due to the no-electrode gaps in the PMN-33%PT plates. It shows high shear stress sensitivity, though, due to high piezoelectric charge constant (d_{31}=-1330 pC/N) of PMN-33%PT single crystal and small thickness of the piezo-plates (=0.5 mm). The sensor yielded almost zero output under the normal stress (about 1-1.3 % of the shear sensitivity), which is well associated to the theoretical prediction that normal

stress should be zero due to the electromechanical symmetry of the bimorph plates. Usable frequency range of sensor was also measured, which shows 0-800 Hz wide range in usage.

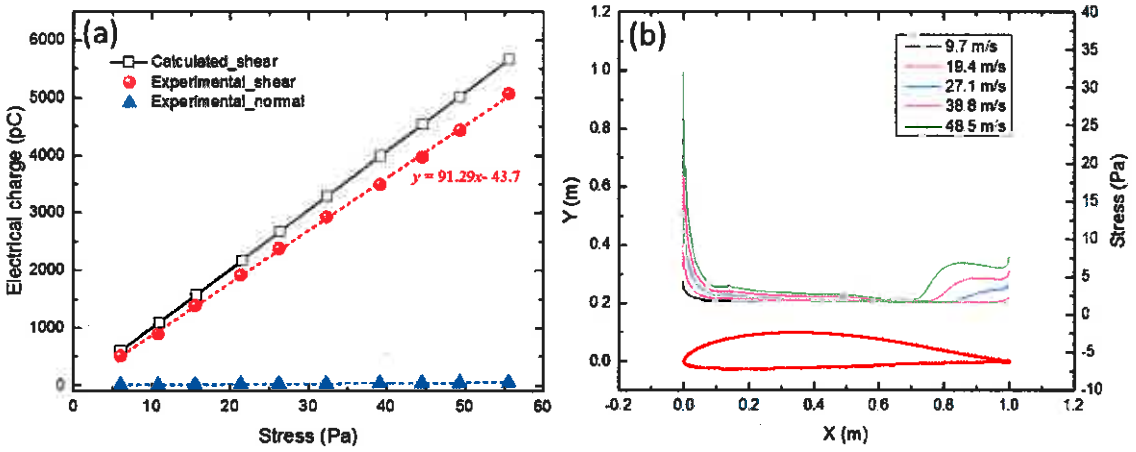

Figure 5. (a) Calculated and measured electrical charge output as a function of shear/normal stress, (b) shear stress distribution on the airfoil as a function of air flow velocity

5. CONCLUSION

In this work, the piezoelectric floating element sensor was designed to minimize the misalignment error considering the gap and lip size of the sensor. The sensor was also designed to be unaffected by normal stresses generated from the vortex lift up so that pure shear stress could be measured. The calibration results showed that the sensor yields high shear stress sensitivity (=91.3 ± 2.1 pC/Pa) due to the high piezoelectric charge constant (d_{31}=-1330 pC/N) of the PMN-33%PT single crystal and small thickness of plates, while showing almost zero charge output under the normal stress. For the future work, this sensor can be flush mounted on an airfoil model for subsonic-wind tunnel-flow measurements.

6. ACKNOWLEDGMENT

This work was supported by National Aeronautics and Space Administration under Grant No. NNX14AN42A.

REFERENCES

[1] Preston, J. P., "The Determination of Turbulent Skin Friction by Means of Pitot Tubes," J. R. Aeronaut. Soc. **58**, 109–121 (1954).

[2] Liu, C., Huang, J. B., Zhu, Z., Jiang, F., Tung, S., Tai, Y. C.., Ho, C. M., "A micromachined flow shear-stress sensor based on thermal transfer principles," J. Microelectromechanical Syst. **8**(1), 90–98 (1999).

[3] Joseph H. Haritonidis., "The measurement of wall shear stress," Adv. Fluid Mech. Meas. **45**, 229–261 (1989).

[4] Schetz, J. A., "Direct Measurement of Skin Friction in Complex Fluid Flows," AIAA 2010-44 (2010).

[5] Heuer, W. D. C.., Marusic, I., "Turbulence wall-shear stress sensor for the atmospheric surface layer," Meas. Sci. Technol. **16**, 1644–1649 (2005).

[6] Desai, a V., Haque, M. a., "Design and fabrication of a direction sensitive MEMS shear stress sensor with high spatial and temporal resolution," J. Micromechanics Microengineering **14**, 1718–1725 (2004).

[7] Padmanabhan, A., Goldberg, H., Breuer, K. D.., Schmidt, M. a., "A wafer-bonded floating-element shear stress microsensor with optical position sensing by photodiodes," J. Microelectromechanical Syst. **5**(4), 307–315 (1996).

[8] Shajii, N. K.., Schmidt, M. A., "A liquid shear-stress sensor using wafer-bonding technology," J. Microelectromechanical Syst. **1**, 89–94 (1992).

[9] Roh, Y. R., "Development of Iocal/global SAW sensors for measurement of wall shear stress in laminar and turbulent flows," Pennsylvania State University (1991).

[10] Roche, D., Richard, C., Eyraud, L.., Audoly, C., "Shear stress sensor using a shear horizontal wave SAW device type on a PZT substrate," Ann. Chim. **20**, 495–498 (1995).

[11] Zhang, R., Jiang, B.., Cao, W., "Elastic, piezoelectric, and dielectric properties of multidomain 0.67Pb(Mg1/3Nb2/3)O3-0.33PbTiO3 single crystals," J. Appl. Phys. **90**(7), 3471–3475 (2001).

[12] Zhang, S., Li, F., Jiang, X., Kim, J., Luo, J.., Geng, X., "Advantages and challenges of relaxor-PbTiO3 ferroelectric crystals for electroacoustic transducers – A review," Prog. Mater. Sci. **68**, 1–66 (2015).

[13] Jiang, X., Kim, J.., Kim, K., "Relaxor-PT Single Crystal Piezoelectric Sensors," Crystals **4**, 351–376 (2014).

[14] Smits, J. G., Dalke, S. I.., Cooney, T. K., "The constituent equations of piezoelectric bimorphs," Sensors Actuators A Phys. **28**, 41–61 (1991).

[15] Roche, D., Richard, C., Eyraud, L.., Audoly, C., "Piezoelectric bimorph bending sensor for shear-stress measurement in fluid flow," Sensors Actuators A Phys. **55**, 157–162 (1996).

[16] Meritt, R. J.., Donbar, J. M., "Error Source Studies of Direct Measurement Skin Friction Sensors," AIAA 2015-1916, 1–20 (2015).

[17] Allen, J. M., "Experimental study of error sources in skin-friction balance measurements," ASME, Trans. Ser. I - J. Fluids Eng. **99**, 197–204 (1977).

[18] Allen, J. M., "An Improved Sensing Element for Skin-Friction Balance Measurements," AIAA **18**(11), 1342–1345 (1980).

[19] O'Donnell, F. B.., Westkaempfer, J. C., "Measurement of Errors Caused by Misalignment of Floating-Element Skin-Friction Balances," AIAA **3**(1), 163–165 (1965).